Cell Host & Microbe
Article

An Intact Cuticle in Distal Tissues Is Essential for the Induction of Systemic Acquired Resistance in Plants

Ye Xia,[1] Qing-Ming Gao,[1] Keshun Yu,[1] Ludmila Lapchyk,[1] DuRoy Navarre,[2] David Hildebrand,[3] Aardra Kachroo,[1,*] and Pradeep Kachroo[1,*]
[1]Department of Plant Pathology, University of Kentucky, Lexington, KY 40546, USA
[2]U.S. Department of Agriculture–Agricultural Research Service, Washington State University, Prosser, WA 99350, USA
[3]Department of Plant Science, University of Kentucky, Lexington, KY 40546, USA
*Correspondence: apkach@uky.edu (A.K.), pk62@uky.edu (P.K.)
DOI 10.1016/j.chom.2009.01.001

SUMMARY

Systemic acquired resistance (SAR), initiated by a plant upon recognition of microbial effectors, involves generation of a mobile signal at the primary infection site, which translocates to and activates defense responses in distal tissues via unknown mechanism(s). We find that an acyl carrier protein, ACP4, is required to perceive the mobile SAR signal in distal tissues of *Arabidopsis*. Although *acp4* plants generated the mobile signal, they failed to induce the systemic immunity response. Defective SAR in *acp4* plants was not due to impairment in salicylic acid (SA)-, methyl SA-, or jasmonic acid-mediated plant hormone signaling pathways but was associated with the impaired cuticle of *acp4* leaves. Other cuticle-impairing genetic mutations or physical removal of the cuticle also compromised SAR. This cuticular requirement was relevant only during mobile signal generation and its translocation to distal tissues. Collectively, these data suggest an active role for the plant cuticle in SAR-related molecular signaling.

INTRODUCTION

The plant cuticle is a hydrophobic layer that covers the aerial surface of plants and forms the first line of contact with the environment. In the epidermis of young leaves, cuticle is present as a highly repellent wax layer, termed procuticle, which matures with the leaf. The mature cuticle is composed of cutin and cuticular wax (Figure S1). In *Arabidopsis*, cutin is a polymer consisting mainly of C16 and C18 diacids and ω- and midchain hydroxy fatty acids (FA) and cuticular wax is a complex mixture of very long chain fatty acid derivatives formed upon elongation of plastidal FAs (reviewed in Pollard et al., 2008). The primary components of *Arabidopsis* leaf waxes are very long chain alkanes and primary alcohols (reviewed in Samuels et al., 2008). The plant cuticle plays an important role in cell-cell interactions such as preventing postgenital organ fusions and mediating pollen-pistil contact (reviewed in Tanaka and Machida, 2006). In addition to limiting nonstomatal water loss, cutin and cuticular wax influence plant-insect interactions and serve as the primary line of defense against pathogens by providing a physical barrier to pathogen ingress (Riederer, 2006).

In addition to this passive defense, plants also induce more specific defense responses targeted to particular pathogens. Often these responses are accompanied by the induction of localized cell death at the site of pathogen entry, which can restrict the spread of the pathogen to cells within and immediately surrounding the lesions. This phenomenon known as the hypersensitive response (HR) is one of the earliest visible manifestations of induced defense response and resembles programmed cell death in animals (Gray, 2002; Glazebrook, 2005; Kachroo and Kachroo, 2006; Thomma et al., 2001). Concurrent with HR development, defense reactions are triggered in sites both local and distal from the primary infection. This phenomenon, known as systemic acquired resistance (SAR), is accompanied by a local as well as systemic increase in endogenous salicylic acid (SA) and the concomitant upregulation of a large set of defense genes, including genes that encode pathogenesis related (PR) proteins (Durrant and Dong, 2004).

SAR involves the generation of a mobile signal in the primary leaves, which when translocated to distal portions of the plant activates defense responses resulting in broad-spectrum disease resistance. The production of mobile signal takes places within 3–6 hr after inoculation of the avirulent pathogen in the primary leaves (Smith-Becker et al., 1998) and the inoculated leaf must remain attached for at least 4 hr after inoculation for the induction of SAR (Rasmussen et al., 1991). Mutations compromising SA/jasmonic acid (JA) synthesis or those impairing SA/JA defense signaling pathways abolish SAR (Durrant and Dong, 2004; Truman et al., 2007). SAR is also dependent on the SA-binding protein 2 (SABP2)-catalyzed conversion of methyl SA to SA in the distal tissues (Kumar and Klessig, 2003). Recent studies have suggested that methyl SA is the mobile signal required to initiate SAR in distal tissues (Park et al., 2007). The generation and/or subsequent translocation of the mobile signal require functions of a putative lipid transfer protein (Maldonado et al., 2002) and glycerol-3-phosphate (G3P) dehydrogenase (G3Pdh; Nandi et al., 2004). The G3Pdh (GLY1) reduces dihydroxyacetone phosphate to generate G3P (Kachroo et al., 2004), an obligatory component and precursor for the biosynthesis of all plant glycerolipids. Although several

components contributing to SAR have been identified, the molecular signaling underlying SAR still remains obscure. Furthermore, the steps or components involved in decoding of the mobile signal remain unknown.

Here, we report the isolation of a component that is essential for SAR mobile signal perception. *Arabidopsis* mutants defective in acyl carrier protein (acp) 4 are able to generate the mobile SAR signal but unable to perceive it and are thereby compromised in the onset of SAR. This defect in SAR is associated with the malformed cuticle of *acp4* leaves. SAR is also compromised in *lacs2*, *lacs9*, *cer1*, *cer3*, and *cer4* mutants, which have permeable cuticles, as well as in wild-type plants where the cuticle is mechanically damaged. Our results suggest that perception of the mobile signal by the cuticle in distal leaves is as important as its generation at the site of primary infection.

In addition to its role in SAR, a mutation in *acp4* also suppresses the altered defense phenotypes observed in *ssi2* mutants. A mutation in the *SSI2* encoded stearoyl-acyl carrier protein-desaturase (SACPD) reduces oleic acid (18:1) levels and triggers constitutive defense signaling by inducing the expression of multiple resistance (*R*) genes (Chandra-Shekara et al., 2007) (Figure S1). The low 18:1-mediated global induction of *R* genes confers broad-spectrum disease resistance to multiple pathogens in *Arabidopsis* and soybean (Kachroo et al., 2001, 2003, 2004, 2005, 2007, 2008). Restoring 18:1 levels in *ssi2* plants by second site mutations in *ACT1* encoded G3P acyltransferase (Kachroo et al., 2003) or *gly1* (Kachroo et al., 2004) suppresses all the *ssi2*-triggered phenotypes. A mutation in *acp4* also restores *ssi2*-triggered phenotypes by restoring 18:1 levels. We show that ACP4 is specifically required for FA biosynthesis in leaves and a mutation in *ACP4* increases 18:1 levels by affecting the ACT1-catalyzed acylation of G3P.

RESULTS

Isolation of the *acp4* Mutant

To identify components mediating 18:1-derived signaling, we carried out a T-DNA based suppressor screen in *Arabidopsis*. The *ssi2* plants were transformed with the pBAR1 vector to generate ~2500 T_1 plants. These were selfed and analyzed in the T_2 generation to identify two putative suppressor mutants that showed WT-like morphology as opposed to the stunted *ssi2* plants. One of these, a pale-colored mutant, designated *ssi2 acp4*, was further analyzed. As opposed to *ssi2*, the *ssi2 acp4* plants did not develop visible or microscopic cell death (Figures 1A and 1B), and were restored in their 18:1 content (Figure 2A, Table S1). Consequently, *ssi2 acp4* plants showed basal expression of *R* and *PR-1* genes and did not accumulate increased salicylic acid (SA) or its glucoside conjugate (SAG) (Figures 1C–1E and S2). Unlike *ssi2*, the *ssi2 acp4* plants were responsive to JA and were able to induce *PDF1.2* expression in response to JA treatment (Figure 1F). Together, these data suggested that the mutation in *ACP4* restored 18:1 levels in *ssi2* plants. This in turn restored all the altered phenotypes of *ssi2* plants, including SA levels.

Analysis of the F2 progeny derived out of a backcross between *ssi2 acp4* with Nössen (WT ecotype) revealed that the *acp4* and *ssi2* mutations segregated independent of each other and the pale phenotype was associated with presence of the *acp4* mutation. Southern analysis showed that both *acp4* and *ssi2 acp4* plants contained a single T-DNA insertion (Figure S3A). This was further confirmed by genetic studies, which mapped the *acp4* mutation to the upper arm of chromosome 4. Attempts to clone the *ACP4* gene using asymmetric or inverse PCR were unsuccessful; therefore, we used map-based cloning and identified that the T-DNA was inserted in a gene encoding *a*cyl *c*arrier *p*rotein *4* (At4g25050, Figure 1G). As predicted, genomic DNA PCRs using *ACP4* gene-specific primers amplified ~1.4 kb from the WT genome but >10 kb product from *acp4* and *ssi2 acp4* plants (Figure 1H, data shown for *ssi2 acp4*). The *ACP4* gene is predicted to encode a mature protein of 89 amino acids (aa), and the T-DNA was inserted after the sixty-first aa. If expressed, the truncated acp4 protein would be translated as the first 61 aa of ACP4 fused to 6 aa derived from the T-DNA sequence. Northern blot analysis was unable to detect full-length or truncated ACP4 transcripts in *acp4* and *ssi2 acp4* plants (Figure 1I), suggesting that the truncated transcript in the *acp4* mutant is either expressed at very low levels or is highly unstable. Expressing a ~3.2 kb genomic sequence spanning the *ACP4* coding region with its native promoter and terminator, showed that the WT *ACP4* gene complemented all the altered phenotypes in transgenic *acp4* and *ssi2 acp4* plants. Thus, the complemented *acp4* and *ssi2 acp4* plants showed WT-like or *ssi2*-like phenotypes, respectively (Figure 1J, data not shown), and the WT-like phenotype segregated with the presence of the transgene in the T2 generation (Figure S3B).

A Mutation in *acp4* Impairs ACT1-Catalyzed Acyltransferase Reaction

FA profiling showed reduced levels of 16:3 in *acp4* and *ssi2 acp4* plants (Table S1, Figure 2A). This was consistent with the suggested role of ACPs in plastidial FA biosynthesis (Browse and Somerville, 1991). Lipid profiling showed that both *acp4* and *ssi2 acp4* plants accumulated significantly reduced amounts of major plastidal lipids including monogalactosyldiacylglycerol, digalactosyldiacylglycerol, and phosphatidylglycerol (Figure 2B), further confirming that a mutation in *acp4* compromised the plastidal pathway for lipid biogenesis. This impairment reduced the overall lipid content in *acp4* and *ssi2 acp4* plants, with the latter accumulating the lowest amounts (nmole per mg dry weight) (Figure 2C). Based upon the comparable lipid profiles of *acp4* and *act1* plants (Kachroo et al., 2005), and the fact that both *act1* and *acp4* mutations suppressed *ssi2*-associated phenotypes, we hypothesized that the *acp4* mutation might impair the G3P acyltransferase (ACT1)-catalyzed reaction. We tested this by comparing phosphatidic acid (PA) levels in *act1* and *acp4* plants, since plastidial PA synthesis relies upon the activity of ACT1 (Kunst et al., 1988). Indeed, *act1* plants showed a significant reduction in PA levels (Figure 2D). Consistent with our hypothesis, PA levels in *acp4* plants were also reduced and only marginally higher compared to those in *act1* plants. Further evidence supporting our hypothesis was obtained by comparing the response of *acp4, act1*, and WT plants to glycerol treatment. Exogenous application of glycerol increases the endogenous G3P levels (Aubert et al., 1994; Chanda et al., 2008), which in turn quench 18:1, producing *ssi2*-like phenotypes in WT plants (Kachroo et al., 2004, 2005). Since *act1* plants are impaired in the acylation of G3P with 18:1 (Kunst et al., 1988),

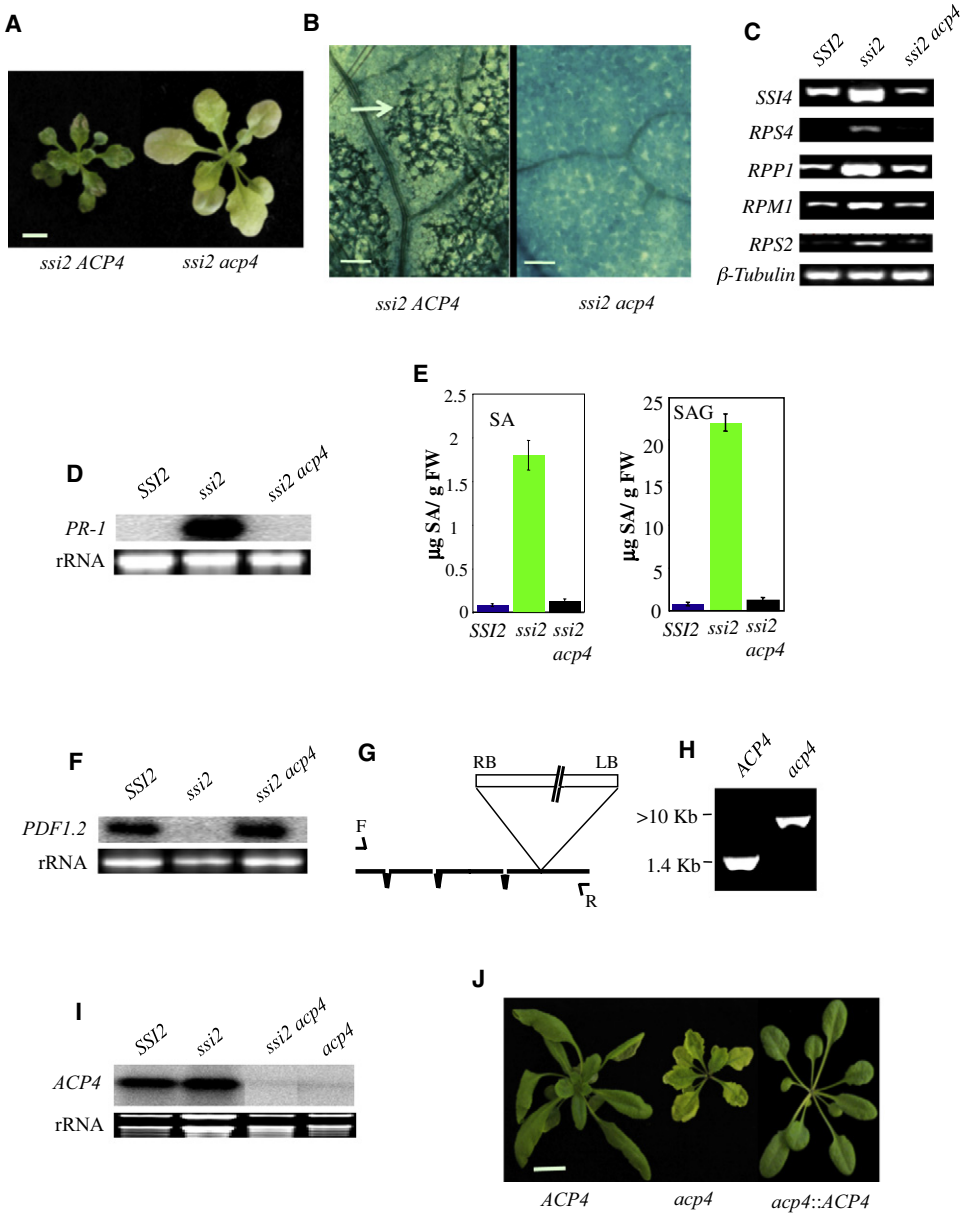

Figure 1. Effect of the *acp4* Mutation on *ssi2* and Wild-Type Plants

(A) Morphological phenotype of 3-week-old *ssi2 ACP4* and *ssi2 acp4* plants (scale, 0.5 cm).

(B) Microscopy of trypan blue stained leaves (scale bars, 270 microns). Arrow indicates dead cells.

(C) RT-PCR analysis showing expression levels of indicated *R* genes.

(D) RNA gel blot showing transript levels of *PR-1* gene.

(E) SA and SAG levels in indicated genotypes.

(F) RNA gel blot showing levels of *PDF1.2* in plants treated with JA for 48 hr.

(G) Structure of *ACP4* gene showing the location of T-DNA insertion. Lines indicate exons and inverted open triangles indicate introns. RB and LB indicate right and left borders of T-DNA, respectively. F and R indicate forward and reverse primer sites used for PCR.

(H) Genomic DNA PCR using *ACP4* gene specific primers shown in (G).

(I) RNA gel blot showing transcript levels of *ACP4* gene.

(J) Morphological phenotype of 3-week-old *ACP4*, *acp4*, or complemented *acp4* (*acp4*::*ACP4*) plants (scale bars, 1 cm).

they remain unaffected upon glycerol treatment (Chandra-Shekara et al., 2007; Kachroo et al., 2004, 2005). Congruent to our hypothesis and in contrast to WT plants, exogenous application of glycerol did not decrease (10 mM) or only nominally decreased (20 or 50 mM glycerol) 18:1 levels in *acp4* plants (Figure 2E). Exogenous application of glycerol (10, 20, and 50 mM) also failed to decrease 18:1 levels in *act1* plants (data not shown) (Kachroo et al., 2004). The degree of 18:1 reduction also correlated with

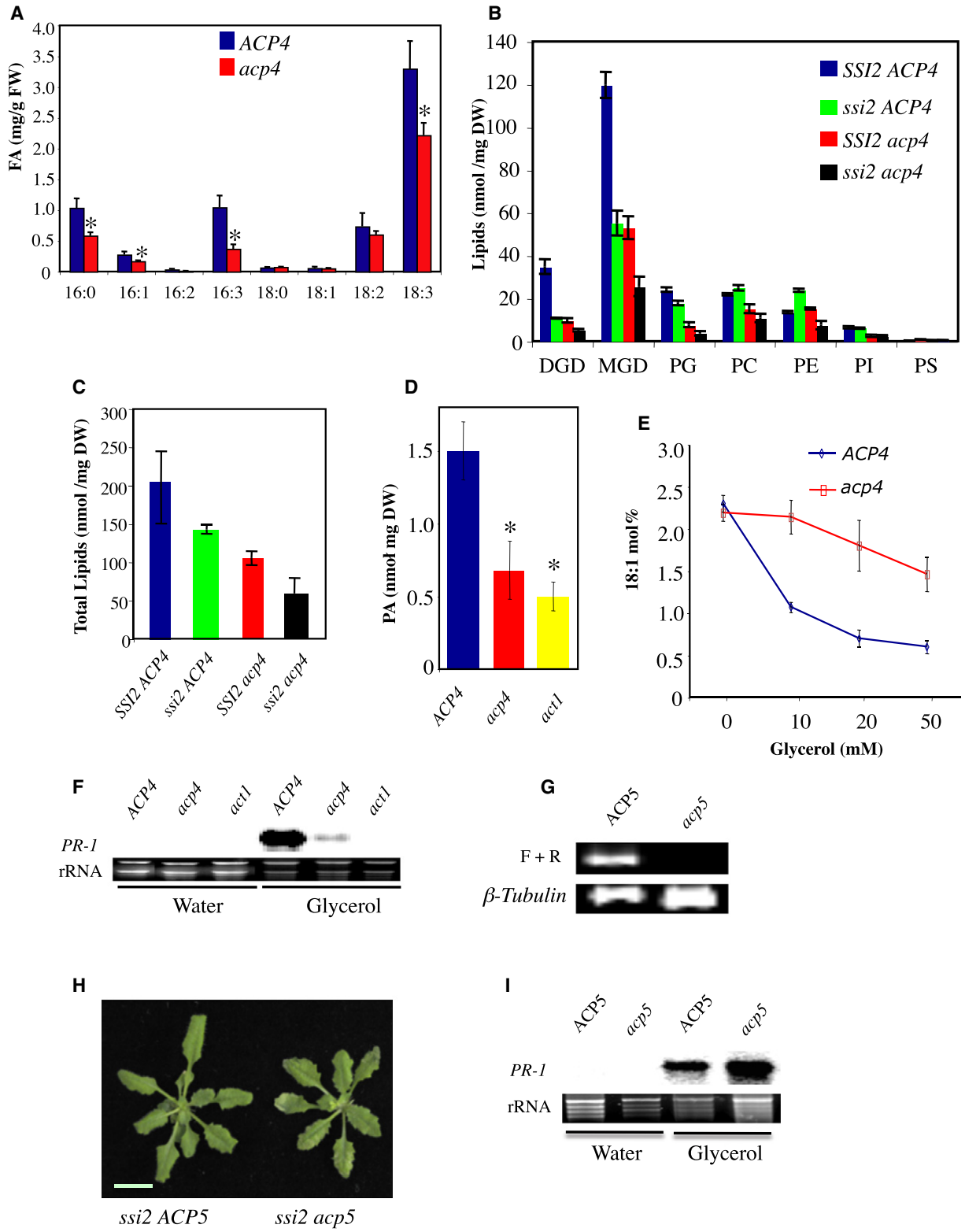

Figure 2. FA, Lipid Profile, Phosphatidic Acid Levels, Glycerol-Induced Decrease in 18:1 Levels, *PR-1* Gene Expression, and Analysis of *acp5* Plants

(A) Levels of FAs in 4-week-old *ACP4* (Nössen) or *acp4* leaves. The error bars represent SD. Asterisks denote a significant difference with WT (t test, $p < 0.05$). FW indicates fresh weight.

PR-1 induction; 50 mM glycerol induced *PR-1* to high levels in WT plants, very low levels in *acp4* plants, but not in *act1* plants (Figure 2F). Together, these results showed that *acp4* plants were partially tolerant to glycerol. This suggested that, although the *Arabidopsis* genome encodes for six different ACP proteins (Table S2), 18:1-ACP4 might be the preferred substrate for the ACT1-catalyzed reaction. A precedent for this is the fact that different G3P acyltransferases exhibit preferences for specific ACP isoforms in spinach (Guerra et al., 1986). We conclude that the increased 18:1 levels and associated suppression of *ssi2* phenotypes in *ssi2 acp4* plants is likely due to impaired ACT1-catalyzed step.

A Mutation in *ACP5* Does Not Rescue *ssi2* Phenotypes

In addition to ACP4, the *Arabidopsis* genome encodes five other ACPs, which encode proteins ranging from 123 to 140 amino acids and show high levels of homology to each other (Table S2). The *ACP2*, *ACP3*, and *ACP5* isoforms showed similar transcript levels in leaf, stem, flower, and root, and their expression in leaves was comparable to that of *ACP4* (Figure S4A). To determine if mutations in other ACP isoforms produced an effect similar to that seen in *acp4*, we screened the SALK insertional database and isolated lines containing homozygous T-DNA insertion within the *ACP5* isoform. The *ACP5* gene is predicted to encode a mature protein of 86 aa, and the T-DNA was inserted after the codon encoding the twenty-first aa. As predicted, genomic or RT-PCR using *ACP5* gene-specific primers did not amplify a product in *acp5* plants (Figure 2G). The *acp5* plants showed WT-like morphology and FA profile (Figure S4B, Table S1). We next crossed *acp5* with *ssi2* and obtained *acp5 ssi2* plants. These double mutant plants showed *ssi2*-like morphology (Figure 2H), constitutive cell death, and increased expression of *PR-1* gene (data not shown). A mutation in *acp5* did not alter the PA levels (data not shown) and the mutant plants also showed WT-like response to exogenous application of glycerol; the decline in 18:1 and induction of *PR-1* gene were similar to WT plants (Figure 2I). Together, these data suggest that the ACP5 isoform does not play a major role in leaf FA synthesis and that a mutation in the *ACP5* isoform does not affect the ACT1-catalyzed step.

A Mutation in *acp4* Compromises SAR

During our analysis of *ssi2 acp4* plants, we noticed that these showed unusually high susceptibility to an avirulent strain of the bacterial pathogen, *Pseudomonas syringae* (*AvrRPT2*) (Figure 3A). Similarly, *acp4* plants also showed enhanced susceptibility to virulent as well as avirulent pathogens expressing *AvrRPT2* (Figure 3B) or *AvrRPS4* (data not shown). Since structurally divergent R proteins (RPS2 and RPS4, respectively) in the host mediate resistance against bacteria expressing *AvrRPT2* or *AvrRPS4*, it appears that a requirement for ACP4 in *R* gene-mediated resistance to avirulent pathogens is independent of the R protein structure. We next tested the ability of *acp4* plants to induce SAR. The plants were first inoculated with $MgCl_2$ or an avirulent strain of *P. syringae* (*AvrRPT2*) and 48 hr later systemic leaves of all plants were challenged with a virulent strain of *P. syringae* (DC3000). The proliferation of virulent bacteria was monitored at 0, 3, and 6 dpi. The WT plants, inoculated first with an avirulent strain, showed ~10-fold reduced growth of virulent bacteria compared to plants whose primary leaves were infiltrated with $MgCl_2$ (Figure 3C). In contrast, the *acp4* plants showed only ~1- to 1.5-fold reduction in the growth of virulent bacteria at 6 dpi, when pre-exposed to avirulent bacteria. Similar results were obtained when WT and *acp4* plants were inoculated with an avirulent stain containing *AvrRPS4* followed by infection with virulent bacteria (Figure S5A).

This defect in SAR was not due to impairments in SA- or JA-mediated signaling, since *acp4* plants not only accumulated WT-like levels of SA and JA in response to pathogen infection (Figures 3D and 3E), but were also responsive to these phytohormones (Figures 3F and 3G). The *acp4* plants were also responsive to methyl SA (MeSA) (Figure 3H), which was recently shown to act as a mobile SAR signal in tobacco (Park et al., 2007). Furthermore, since MeSA is biologically inactive (Seskar et al., 1998), it appears that *acp4* plants are not impaired in the conversion of MeSA to SA, a reaction essential for the onset of SAR in systemic leaves (Park et al., 2007). These results suggest that *acp4* plants are impaired in their ability to synthesize, transduce, or perceive a mobile signal that triggers SAR.

To test if *ACP4* participated in mobile signal generation, we evaluated the response of WT and *acp4* plants to phloem exudates collected from WT or *acp4* petioles. The WT and *acp4* leaves were infiltrated with $MgCl_2$ or *P. syringae* containing *AvrRPT2*. Petiole exudates collected from the inoculated leaves were injected into the leaves of WT or *acp4* plants. The exudate-injected leaves were then analyzed for the expression of the SAR marker gene, *PR-1*. Interestingly, petiole exudates from pathogen inoculated WT as well as *acp4* plants induced *PR-1* gene expression in WT leaves but not in *acp4* leaves (Figure 3I). We next determined whether this inability to induce *PR-1* in response to exudates correlated with an impaired pathogen response in *acp4* plants. Petiole exudates from WT and *acp4* plants inoculated with $MgCl_2$ or *P. syringae*-containing *AvrRPT2* were infiltrated into WT or *acp4* leaves. Systemic leaves of the infiltrated plants were then inoculated with virulent pathogen, and proliferation of virulent pathogen was monitored at 0 and 3 dpi (Figure 3J). As expected, exudates collected from WT plants inoculated with avirulent pathogen conferred

(B) Profile of total lipids extracted from wild-type (*SSI2 ACP4*), *ssi2*, *acp4*, and *ssi2 acp4* plants. The values are presented as a mean of five replicates. The error bars represent SD. Symbols for various components are the following: DGD, digalactosyldiacylglycerol; MGD, monogalactosyldiacylglycerol; PG, phosphatidylglycerol; PC, phosphatidylcholine; PE, phosphatidylethaloamine; PI, phosphatidylinositol; PS, phosphatidylserine.
(C) Total lipid levels in indicated genotypes. DW indicates dry weight.
(D) Phosphatidic acid (PA) levels in indicated genotypes. Asterisks denote a significant difference with WT (t test, $p < 0.05$).
(E) 18:1 levels in *ACP4* or *acp4* plants treated with indicated concentrations of glycerol.
(F) RNA gel blot showing transcript levels of *PR-1* gene in indicated genotypes 72 hr after water or 50 mM glycerol treatments.
(G) RT-PCR analysis showing *ACP5* transcript levels.
(H) Morphological phenotype of 4-week-old *ssi2* and *ssi2 acp5* plants (scale bar, 0.5 cm).
(I) RNA gel blot showing transcript levels of *PR-1* gene in indicated genotypes 72 hr after water or 50 mM glycerol treatments.

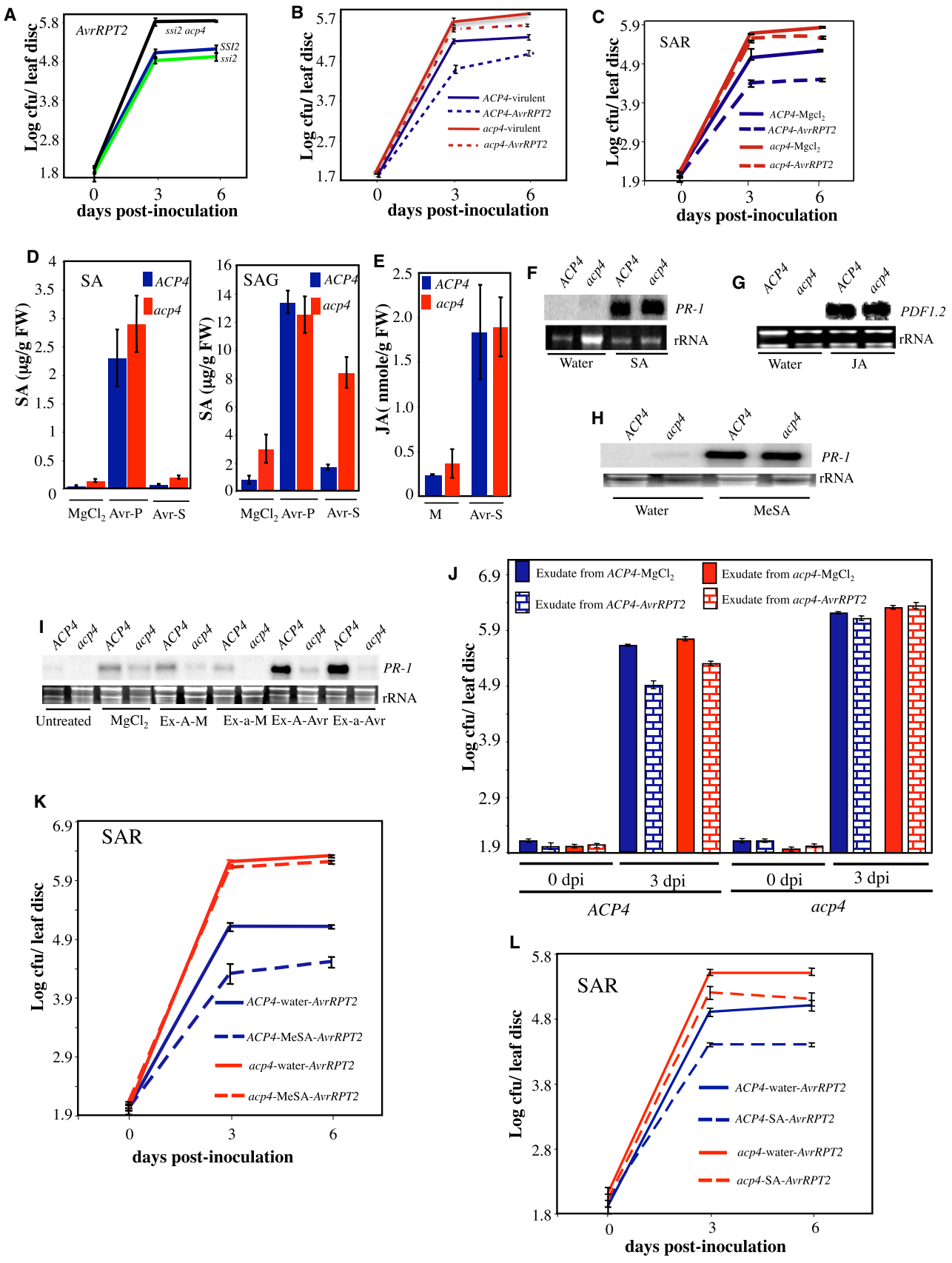
A
AvrRPT2
ssi2 acp4
SSI2
ssi2
Log cfu/ leaf disc
days post-inoculation
B
ACP4-virulent
ACP4-AvrRPT2
acp4-virulent
acp4-AvrRPT2
C
SAR
ACP4-MgCl2
ACP4-AvrRPT2
acp4-MgCl2
acp4-AvrRPT2
D
SA
SAG
SA (µg/g FW)
MgCl2 Avr-P Avr-S
E
JA(nmole/g FW)
M Avr-S
F
PR-1
rRNA
Water SA
G
PDF1.2
Water JA
H
Water MeSA
I
Untreated MgCl2 Ex-A-M Ex-a-M Ex-A-Avr Ex-a-Avr
J
Exudate from ACP4-MgCl2
Exudate from acp4-MgCl2
Exudate from ACP4-AvrRPT2
Exudate from acp4-AvrRPT2
0 dpi 3 dpi 0 dpi 3 dpi
ACP4 acp4
K
SAR
ACP4-water-AvrRPT2
ACP4-MeSA-AvrRPT2
acp4-water-AvrRPT2
acp4-MeSA-AvrRPT2
L
SAR
ACP4-water-AvrRPT2
ACP4-SA-AvrRPT2
acp4-water-AvrRPT2
acp4-SA-AvrRPT2

protection against virulent pathogen in WT plants. However, exudates collected from WT plants inoculated with avirulent pathogen failed to protect *acp4* plants from the virulent pathogen. Similarly, exudates collected from *acp4* plants inoculated with avirulent pathogen conferred SAR on WT plants but not on *acp4* plants. Together, these results suggested that although *acp4* plants are competent in generating the mobile SAR signal, they are incapable of responding to this signal.

We next tested if pretreatment with SA, MeSA, or JA bolstered the ability of *acp4* plants to induce SAR. Plants were pretreated with water, SA, MeSA, or JA for 48 hr prior to inoculation with $MgCl_2$ or avirulent bacteria, and 48 hr later systemic leaves of all plants were challenged with a virulent strain of *P. syringae*. Pretreatment with MeSA or JA showed marginal or no improvement in SAR response in *acp4* plants (Figures 3K [data not shown for $MgCl_2$ infiltrated leaves] and S5B). In comparison, pretreatment with SA showed nominal improvement in SAR, although the pathogen growth in SA-treated *acp4* plants was higher compared to water-treated WT plants (Figure 3L, data not shown for $MgCl_2$ infiltrated leaves). Pretreatment of only the primary leaf with SA did not improve the SAR response in *acp4* plants (data not shown). Together, these results suggest that the prior induction of SA-mediated defenses can partially compensate for an impaired cuticle during SAR.

The *acp4* Plants Are Impaired in Cuticular Wax and Cutin Formation

Examination of leaf morphology of *acp4* plants revealed chlorotic patches that showed increased prominence in older leaves (data not shown). To test if the altered leaf phenotype of *acp4* plants was due to a defect in the cuticle, which forms the outermost structure of the leaves (Samuels et al., 2008), we stained WT and *acp4* leaves with toluidine blue, a hydrophilic dye that only penetrates leaves with permeable cuticles (Tanaka et al., 2004). Toluidine blue rapidly penetrated *acp4* leaves, staining these blue, suggesting cuticular permeability (Figure 4A). This was further supported by the rapid leaching of chlorophyll from *acp4* leaves (Figure 4B). Likewise, *acp4* leaves lost more water when subjected to drought stress (data not shown).

To prove that the cuticle is indeed impaired in *acp4* leaves, we analyzed the outermost cell wall of the epidermis by transmission electron microscopy (TEM). As expected, the cuticle of the wild-type leaf appeared as a continuous and regular electron-dense osmiophilic layer outside the cell wall (Figure 4C, marked by a red arrow). In comparison, *acp4* mutant showed an electron-opaque cuticle. The electron-opaque regions were also observed underneath the cuticle and within the outermost layer of the cell wall (Figure 4C, marked by black arrows). Comparison of the scanning electron micrographs (SEM) of WT and *acp4* leaf surfaces showed that both adaxial and abaxial surfaces of *acp4* leaves were stretched and ruptured (Figure 4D).

To determine if this defect in cuticle structure was associated with alterations in the content and/or composition of cuticular waxes or cutin polyester monomers, we compared levels of waxes and cutin monomers between WT and *acp4* leaves. The *acp4* leaves showed reduced levels of FA, alkanes and primary alcohols compared to WT plants (Figure 4E). Similarly, the *acp4* leaves also showed a ~55% overall decrease in cutin aliphatic monomer content (Figure 4F). The decrease was more pronounced in two major monomers (16:0- and18:2-dicarboxylic acids [DCA]). Taken together, these results show that ACP4 is essential for the biosynthesis of the cuticular wax and cutin polymers in leaves.

We next compared SEM of the surface of WT and *acp4* stems to determine if ACP4 was also required for epicuticular wax crystalloid formation (Figure S4E). The structure and the density of the wax crystalloids on *acp4* were similar to that seen on the WT stems, suggesting that the *acp4* mutation did not impair stem cuticle. This was further corroborated by toluidine blue staining and FA analysis; no significant differences were observed between WT and *acp4* stems (Table S1, data not shown). Furthermore, FA analysis of seed, silique, root, and flower tissues from *acp4* plants showed WT-like profiles (data not shown). Together, these data suggest that the *acp4* plants are specifically defective in the leaf cuticle.

To determine if a defect in cuticle correlated with cell-type-specific expression of *ACP4* in the leaf tissue, we generated transgenic lines expressing *β-glucuronidase* (GUS) under the control of *ACP4* promoter. The histochemically stained leaves were fixed, sectioned, and examined by light microscopy. GUS activity was detected throughout the leaf, although maximum activity was detected in vascular tissues and trichomes (Figure S4C). This result suggests that ACP4 functions are likely not restricted to the synthesis of cuticular components in the epidermal layer and that ACP4 is likely involved in general FA and lipid synthesis, which is highest in the leaf mesophyll

Figure 3. Pathogen Resistance; Pathogen-Induced SA and JA Levels; and SA, MeSA, JA, and Exudate Responsiveness

(A) Growth of avirulent *P. syringae* on leaves from indicated genotypes.

(B) Growth of virulent or avirulent (*AvrRPT2*) *P. syringae* strains on *ACP4* or *acp4* leaves.

(C) SAR in *ACP4* or *acp4* plants.

(D) SA and SAG levels in mock- ($MgCl_2$) or pathogen-inoculated primary (Avr-P) or systemic (Avr-S) leaves 48 hr after inoculation with avirulent pathogen.

(E) JA levels in mock- or pathogen-inoculated systemic leaves (Avr-S) 6 hr after inoculation with avirulent pathogen.

(F) RNA gel blot showing transcript levels of *PR-1* gene in plants treated with water or SA for 48 hr.

(G) RNA gel blot showing transcript levels of *PR-1* gene in plants treated with water or JA for 48 hr.

(H) RNA gel blot showing transcript levels of *PR-1* gene in plants treated with water or MeSA for 48 hr.

(I) RNA gel blot showing transcript levels of *PR-1* gene in untreated or treated leaves of *ACP4* (A) and *acp4* (a). Leaves were infiltrated either with $MgCl_2$ or petiole exudates (Ex) and analyzed for *PR-1* transcript levels 48 hr after treatments. M and Avr indicate petiole exudates collected from leaves infiltrated with $MgCl_2$ or *P. syringae* containing *AvrRPT2*.

(J) SAR response in WT (*ACP4*) and *acp4* plants infiltrated with exudates collected from WT or *acp4* plants that were treated either with $MgCl_2$ or *AvrRPT2*.

(K) SAR in *ACP4* or *acp4* plants treated with water (solid lines) or MeSA (dashed lines) for 48 hr prior to inoculation.

(L) SAR in *ACP4* or *acp4* plants treated with water (solid lines) or SA (dashed lines) for 48 hr prior to inoculation. Primary leaves in (K) and (L) were inoculated with $MgCl_2$ (not shown in the figure) or *P. syringae* containing *AvrRPT2*, and the systemic leaves were inoculated with a virulent strain of *P. syringae*. The error bars represent SD.

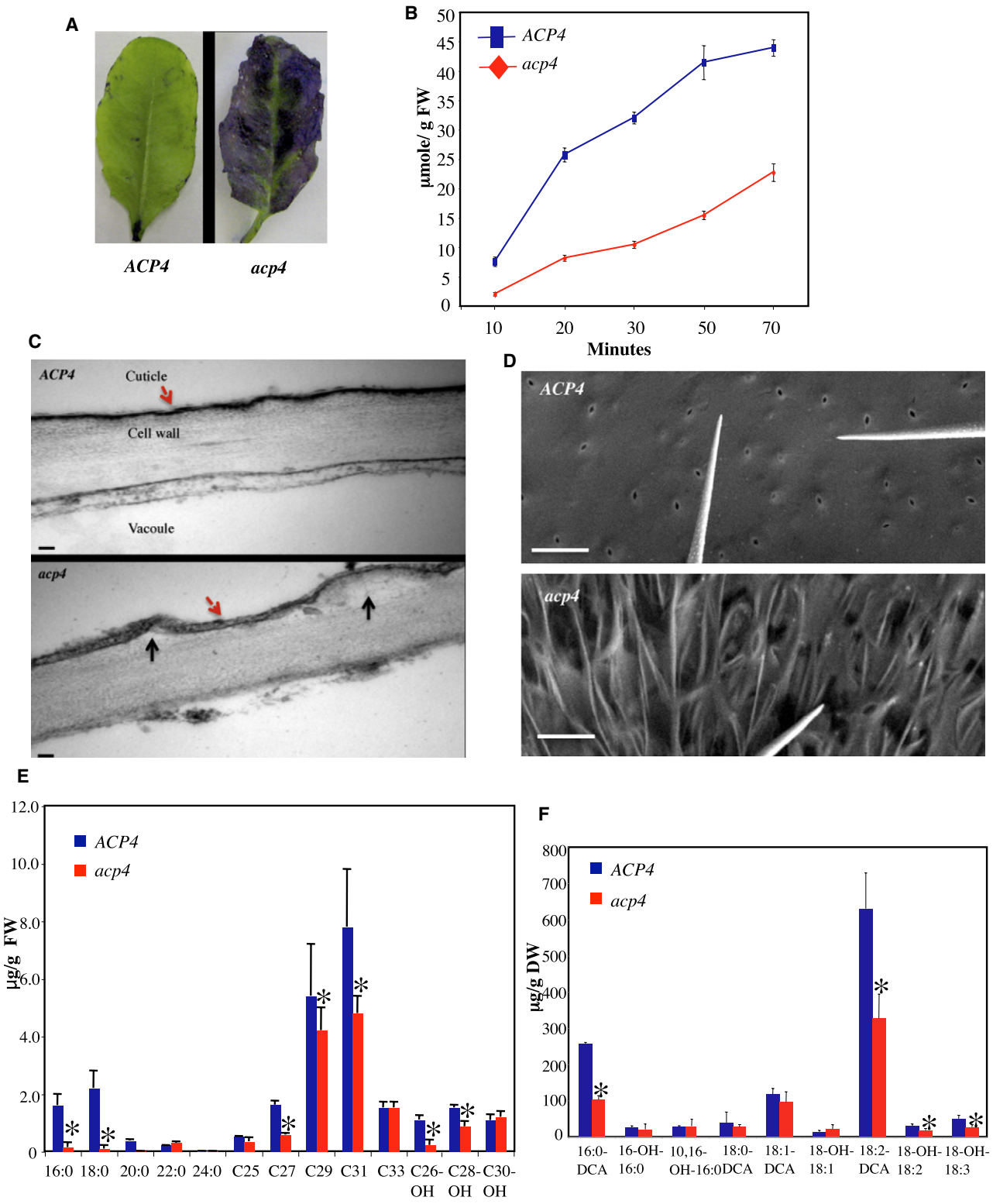

Figure 4. Evaluation of Cuticle-Associated Phenotypes in *acp4* Plants

(A) Toluidine blue stained leaves from 4-week-old leaves of *ACP4* or *acp4* plants.

(B) A time-course measurement of chlorophyll leaching in *ACP4* and *acp4* leaves at indicated times.

(C) Transmission electron micrographs showing cuticle layer on adaxial surface of WT or *acp4* leaves. Red arrow indicates cuticle. Black arrows indicate electron-opaque regions below cuticle layer (scale bars, 50 nm).

tissues. The GUS activity also correlated with *ACP4* expression in various tissues; leaf, stem, and flower tissues showed high *ACP4* transcript and GUS activity but roots showed very low transcript and no GUS activity (Figures S3A and S3D).

Mutations in *lacs2*, *lacs9*, *cer1*, *cer3* (*wax2*), *cer4* Impair SAR

To test the possibility that an intact cuticle was essential for SAR signal perception, we examined the SAR response in mutants known (*lacs2*) (Schnurr et al., 2004), or likely (*lacs9*) (Schnurr et al., 2002) to have defective cuticles. The *LACS* encoded acyl CoA synthetases are enzymes synthesizing the CoA ester formation of fatty acids (Browse and Somerville, 1991; Schnurr et al., 2004). Although the *Arabidopsis* genome encodes nine *LACS* isoforms (Shockey et al., 2002), only *LACS2* has been associated with cutin formation (Schnurr et al., 2004). The *lacs2* mutant was previously reported to show pronounced susceptibility to virulent and avirulent strains of *Pseudomonas* (Tang et al., 2007). Since the *LACS9* gene is involved in the export of FAs, similar to *LACS2* (Schnurr et al., 2002; Schnurr et al., 2004), we hypothesized that it too might participate in cuticle formation. Indeed, both *lacs2-1* and *lacs9-1* leaves showed reduced levels of FAs compared to WT plants (Figure S6A). Furthermore, similar to *lacs2*, *lacs9* mutant stained intensely with toluidine blue (Figure 5A), leached chlorophyll rapidly (Figure 5B), and lost more water upon drought stress (data not shown). These data suggested that, like *lacs2*, a mutation in *lacs9* also altered cuticular permeability. Both *lacs2* and *lacs9* plants supported increased growth of virulent and avirulent *Pseudomonas* strains (Figures 5C and S6B, data not shown for avirulent strain). Notably, not only were *lacs2* and *lacs9* plants impaired in their abilities to induce SAR, but their reduced SAR capabilities were only marginally better than the SAR-impaired *npr1* mutant (Cao et al., 1994).

We next tested SAR in *cer1-1*, *cer3-1* (*wax2*), *cer4-1* mutants, which participate in different steps leading to the biosynthesis of cuticular wax (Samuels et al., 2008). As expected, leaves from all three *cer* mutants stained intensely with toluidine blue (Figure 5A). Control leaves (L*er* ecotype) infiltrated with $MgCl_2$ supported more growth of the secondary virulent pathogen than the plants that were preinfected with an avirulent strain, indicating the appropriate induction of SAR (Figure 5D). In comparison, leaves from *cer* plants infiltrated either with avirulent pathogen or $MgCl_2$ showed similar growth of virulent pathogen. Thus, similar to *lacs2* and *lacs9* plants, all three *cer* mutants tested here showed compromised SAR.

Intact Cuticle Is Specifically Required for SAR and Not for Local Responses

Our data thus far presented a strong correlation between SAR with the presence of an intact cuticle. To further verify if cuticle was required for SAR in WT plants, we damaged the cuticle of WT leaves by mechanical abrasion and tested their ability to induce SAR. Among several methods described for the removal of cuticle (Campbell and McInnes, 1999), we determined that gentle rubbing with a buffered solution containing celite and bentonite was sufficient to damage the cuticle and such leaves stained intensely with toluidine blue (Figure 6A). However, leaves stained 24 hr after mechanical abrasion imbibed significantly less stain, suggesting that the leaves were capable of restoring their damaged cuticle (Figure 6A). These results were further confirmed by TEM analysis; leaves analyzed 1 and 24 hr post abrasion showed electron-opaque and electron-dense cuticles, respectively (Figure 6B). Interestingly, there was a ~2.4 fold increase in the thickness of cell wall 1 hr post abrasion (681.75 ± 24.63 nm). In comparison, leaves analyzed 24 hr postabrasion showed normal thickness of cell wall (277.3 ± 13.3 nm). Analysis of cutin monomers and wax contents did not show a significant difference between treated and untreated leaves (Figures 6C and S7A), suggesting that abrasion was not associated with changes in the composition of cuticular wax or cutin monomers.

To test the requirement of cuticle in SAR, the cuticle was mechanically damaged from the distal leaves at 0, 12, 24, or 42 hr after infiltrating the primary leaves with $MgCl_2$ or an avirulent pathogen. Both control and damaged distal leaves were then inoculated with virulent bacteria 48 hr after infiltration of the primary leaves. The growth of the virulent bacteria was monitored at 0 (white bars) and 3 dpi (blue bars) (Figure 6D). Control plants preinfiltrated with $MgCl_2$ (with intact cuticle) supported more growth of the secondary virulent pathogen than plants that were preinfected with an avirulent strain, indicating the appropriate induction of SAR (Figure 6D). In contrast, distal leaves damaged at 0 or 12 hr after avirulent inoculation supported increased growth of the virulent pathogen (virulent bacteria inoculated 48 and 36 hr post abrasion, respectively) indicating that these were compromised in SAR. On the other hand, distal leaves that were damaged 24 or 42 hr after avirulent inoculation exhibited normal SAR induction (virulent bacteria inoculated 24 and 6 hr post abrasion, respectively). The mechanical abrasion of leaves did not induce the expression of marker genes normally associated with accumulation of reactive oxygen species, SA or JA (Figure S7B), which suggests that abrasion was unlikely to have an effect on SAR response. These results confirmed that an intact cuticle is essential for SAR and showed that the proper onset of SAR requires a cuticle-derived component(s) within 12–24 hr of primary infection.

To determine if cuticle was also required for local responses, we tested the response of WT plants with damaged cuticles to virulent and avirulent (*AvrRPT2*) pathogens. Unlike SAR, cuticular damage did not cause increased susceptibility to either virulent (Figure 6E) or avirulent (Figure S7C) pathogens. Together, these data suggest that cuticle is specifically required for SAR and not for local responses.

(D) Scanning electron micrographs showing adaxial surface of *ACP4* or *acp4* leaves (scale bars, 200 μm).

(E) Analysis of wax components from leaves of 4-week old WT (*ACP4*) and *acp4* plants 16:0-24:0 are FAs, C25-C33 are alkanes, C26-OH-C30-OH are primary alcohols.

(F) Analysis of lipid polyester monomer content of 4-week-old *ACP4* and *acp4* plants. Error bars in (E) and (F) represent SD. Asterisks in (E) and (F) denote a significant difference with WT (t test, $p < 0.05$). Symbols for various components are: 16:0-DCA, 1,16-hexadecane dioic acid; 16-OH-16:0, 16-hydroxyhexadecanoic acid; 10,16-OH-16:0, 10,16-dihydroxyhexadecanoic acid; 18:0-DCA, 1,18-octadecane dioic acid; 18:1-DCA, 1,18-octadecene dioic acid; 18-OH-18:1, 18-hydroxyoctadecenoic acid, 18:2-DCA, 1,18-octadecadiene dioic acid; 18-OH-18:2, 18-hydroxyoctadecadienoic acid; 18-OH-18:3, 18-hydroxyoctadecatrienoic acid.

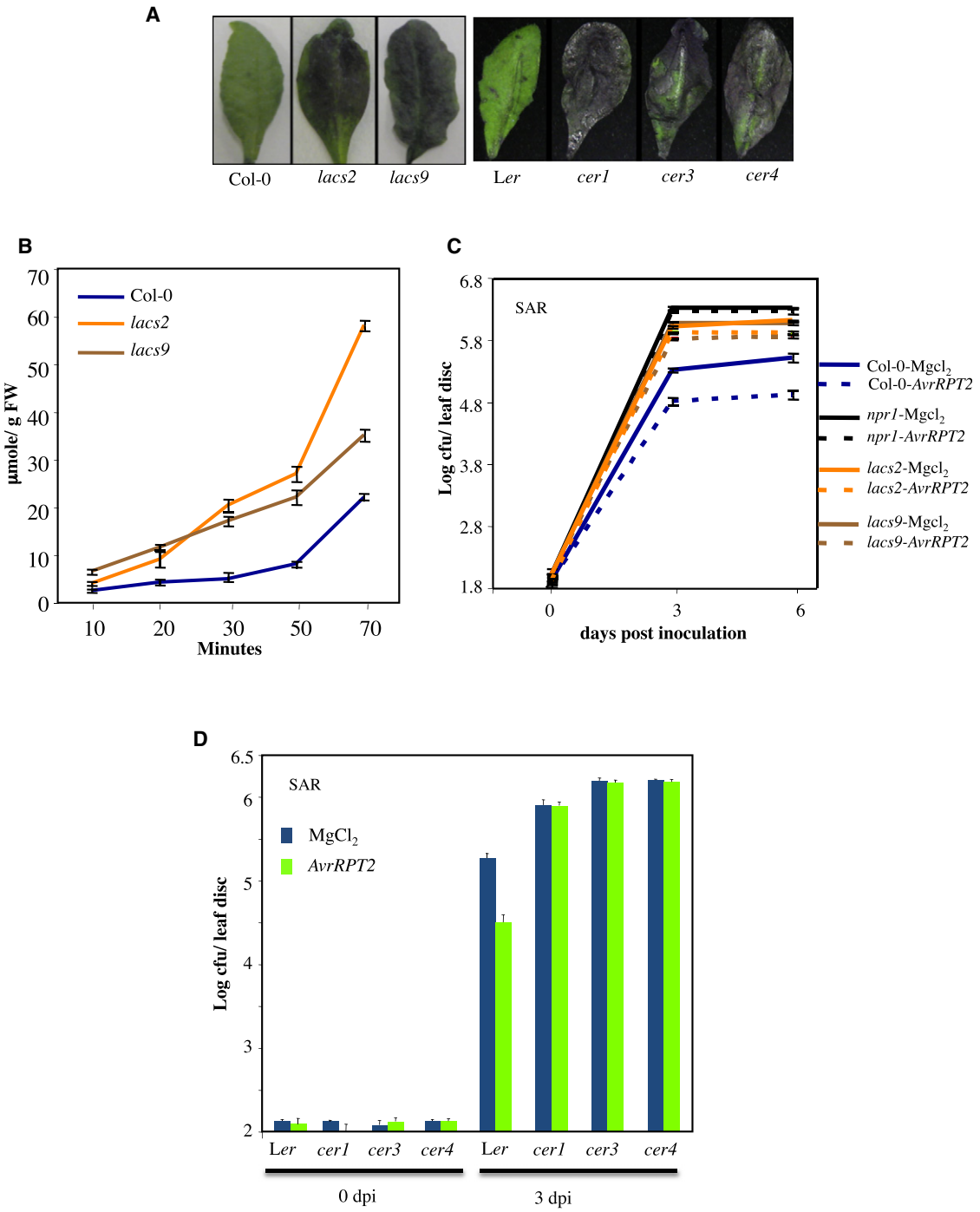

Figure 5. Evaluation of SAR in *lacs2-1*, *lacs9-1*, *cer1-1*, *cer3-1*, and *cer4-1* Plants

(A) Toluidine blue-stained leaves from indicated genotypes.

(B) A time-course measurement of chlorophyll leaching in various genotypes at indicated times.

(C and D) SAR in indicated genotypes.

DISCUSSION

The plant cuticle is primarily viewed as a physical barrier that protects plants from its environment. Recent evidence suggests that the composition of the cuticle affects stomata and trichome development and in addition plays a role in organ fusions (reviewed in Bird and Gray, 2003). For example, epidermal fusion phenotype of the *fdh* mutant has been suggested to be due to a change in the permeability of the cuticle (Lolle et al., 1997). Similarly, diffusion of an unknown inhibitor of guard cells through

the stomata has been proposed to control development of stomata (Bird and Gray, 2003). The lipids present in the outermost layer of pollen grains and the cuticle on the epidermal surface are also suggested to play a direct role in the regulation of water transfer between the pollen grain and stigma surface (Lolle and Pruitt, 1999). More recently, cutin has been associated with basal resistance to necrotrophic pathogens. Both *lacs2* and *gpat4 gpat8* plants are defective in cutin content, but while *lacs2* plants show enhanced resistance to *Botrytis* (Bessire et al., 2007; Tang et al., 2007), *gpat4 gpat8* plants are susceptible to *Alternaria* (Li et al., 2007). These observations, together with our current findings implicate the cuticle in a more active signaling role in plant defense. Systemic immunity in plants not only requires the proper generation and transmittance of a signal at the site of primary infection but also depends upon its reception and decoding in the distal tissues. In this study we demonstrate that the cuticle or a derived component in the distal tissues is required for this perception of the mobile SAR signal. A mutation in ACP4, a critical component of FA biosynthesis, impairs SAR because it affects cuticle formation in the leaf.

The requirement of an intact cuticle for the proper onset of SAR is further reinforced by the observations that genetic mutations (*lacs2*, *lacs9*, *cer1*, *cer3*, and *cer4*) resulting in defective cuticle, as well as mechanically damaging the cuticle of systemic leaves in WT plants, impair SAR. While it is likely that the mechanical removal of cuticle produces effects that are separate from that of genetic mutations affecting cuticle development, it is important to note that SAR was impaired only if the cuticle was removed within 24 hr of primary infection but not after. Previous studies in cucumber have shown that transportation of the mobile signal to distal tissues occurs within 3–5 hr, resulting in defense gene activation within 24 hr of primary infection (Rasmussen et al., 1991; Smith-Becker et al., 1998). This suggests that perception of the mobile signal by the cuticle of systemic tissues is only relevant during the time frame of signal generation in response to primary infection.

WT plants infiltrated with petiole exudates from *Avr*-infected *acp4* leaves induced expression of the SAR marker *PR-1*. However, exudates from *Avr*-infected WT plants failed to induce *PR-1* in *acp4* plants. Furthermore, exudates from *Avr*-infected WT or *acp4* plants induced SAR in WT but not in *acp4* plants. These data suggest that a cuticle-derived component is essential for perception of the mobile signal. However, a role for ACP4-derived factor in mobile signal generation cannot be altogether ruled out since SAR induced in response to exudates from *Avr*-infected *acp4* plants was not exactly comparable to that from WT plants.

A mutation in *acp4* impairs the ACT1-catalyzed acylation of G3P resulting in impaired plastidal lipid biosynthesis. Yet, the *acp4* mutation restored wt-like levels of 18:1 in *ssi2* plants, suggesting that 18:1-ACP4 might serve as the preferred substrate for ACT1. Indeed, with the exception of their cuticles, *acp4* and *act1* plants exhibit comparable phenotypes; mutations in these genes reduce PA levels, confer tolerance to glycerol, impair plastidal lipid synthesis and restore *ssi2* phenotypes. Since *act1* plants are only defective in plastidal lipid biosynthesis and not de novo FA synthesis, they contain WT levels of 16:0, unlike *acp4* plants, which are reduced in 16:0 content. This suggests that the cuticular defect in *acp4* plants may be related to their reduced 16:0 levels. Indeed, 16:0 and 18:0 FAs serve as precursors for the synthesis of very long-chain FAs, which in turn contribute to the synthesis of long-chain aliphatic compounds, the major components of cuticular wax (Samuels et al., 2008). In addition to serving as precursors for glycerolipid synthesis, short-chain FAs produced in plastids also acts as precursors for the synthesis of hydroxy FAs (Figure S1), which form major components of the cutin polyester. Thus, reduced overall FA flux in *acp4* plants is likely responsible for their defective cuticle.

The observation that *acp4* plants are only defective in leaf FA content and cuticlar wax, and not the stem, presents the possibility that different *ACP* isoforms in *Arabidopsis* might serve in FA biosynthesis in specific tissues. It is highly likely that ACP4 is the preferred leaf isoform since it is also the most abundant isoform in leaves (Bonaventure and Ohlrogge, 2002). This tissue-specific preference for different isozymes is reinforced by our findings that a knockout mutation in the related isoform *ACP5* does not result in defects in FA or leaf cuticle, and consequently these plants are not affected in the levels of the ACT1-generated PA or SAR. This and the fact that acyl-ACP desaturases in coriander and *Thunbergia alta* require specific ACP isoforms for optimal activity (Suh et al., 1999) underscore the preferential recruitment of specific ACPs by different FA biosynthetic enzymes.

Notably, *acp4*, *lacs2*, and *lacs9* plants also showed enhanced susceptibility to virulent and avirulent pathogens. However, this enhanced susceptibility cannot be attributed to a defective cuticle as cuticle abrasion did not alter basal or *R* gene-mediated resistance. One common phenotype shared between *acp4*, *lacs2*, and *lacs9* mutants is that they are all compromised in FA/ lipid flux (Figure S6A) Kachroo et al., 2004, 2005). Since FA/lipids serve as an important energy reserve (Somerville and Browse, 1991) and because defense to pathogens is an energy demanding process (Heidel et al., 2004; Heil and Baldwin, 2002), it is plausible that the reduced FA/lipid turnover rate in *acp4*, *lacs2*, and *lacs9* plants make them more vulnerable to virulent/avirulent pathogens. Alternately, a combination of FA/lipid flux, cuticle, or other unknown factors may contribute to basal and *R* gene-mediated resistance to avirulent pathogens. Further biochemical characterization will help unravel the specific role(s) of cuticular components in pathogen resistance and systemic immunity.

EXPERIMENTAL PROCEDURES

Plant Growth Conditions and Genetic Analysis

Plants were grown in MTPS 144 Conviron (Winnipeg, MB, Canada) walk-in chambers at 22°C, 65% relative humidity, and 14 hr photoperiod. The suppressor screen was carried out by transforming *ssi2* plants with the binary vector pBAR1, and the T2 plants were screened for WT-like morphology. The *ssi2 acp4* plants were backcrossed twice and subsequently used for an outcross with Columbia (Col-0) ecotype. A cross between *ssi2 acp4* and Col-0 segregated *acp4*- and *ssi2 acp4*-like plants, and these were distinguished based on the smaller morphology of *ssi2 acp4* plants. Both *acp4*- and *ssi2 acp4*-like F2 plants were used for mapping studies separately.

The SALK insertional line 111501 was screened for the presence of mutant containing a T-DNA insertion in the *ACP5* gene. The *acp5 ssi2* plants were obtained by crossing *acp5* with *ssi2*. The *ACP5* gene specific primers and a left border primer (Table S3) were used to identify the *acp5* homozygous plants.

Complementation Analysis

A ~3.2 kb region encompassing *ACP4*-coding region was amplified from Col-0 genomic DNA using XbaI- and SacI-linkered primers (Table S3) and cloned into the pBAR1 binary vector. The binary vector was transformed

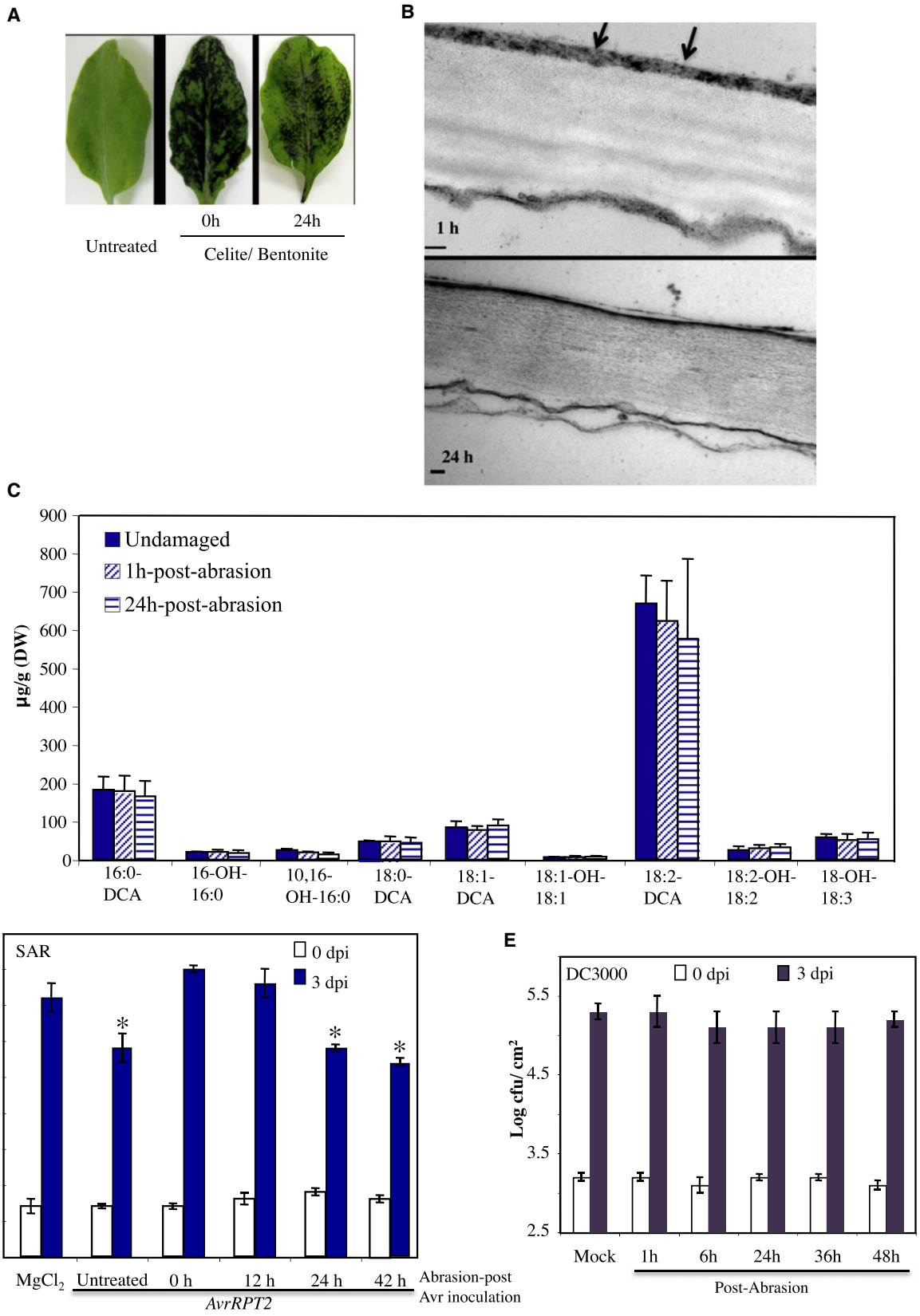
A
0h
24h
Untreated
Celite/ Bentonite
B
1 h
24 h
C
Undamaged
1h-post-abrasion
24h-post-abrasion
µg/g (DW)
16:0-DCA
16-OH-16:0
10,16-OH-16:0
18:0-DCA
18:1-DCA
18:1-OH-18:1
18:2-DCA
18:2-OH-18:2
18-OH-18:3
D
SAR
0 dpi
3 dpi
Log cfu/ cm²
MgCl2
Untreated
0 h
12 h
24 h
42 h
Abrasion-post Avr inoculation
AvrRPT2
E
DC3000
0 dpi
3 dpi
Log cfu/ cm²
Mock
1h
6h
24h
36h
48h
Post-Abrasion

into *acp4* and *ssi2 acp4* plants using floral dip method (Clough and Bent, 1998). The transgenic plants were selected on soil sprayed with the herbicide Basta. Genotype analysis of T-DNA insertion within At4g25050 was carried out using gene-specific and T-DNA left-border specific primers (Table S3).

Histochemical GUS Analysis

A 856 bp portion of the *ACP4* promoter region was amplified by PCR using linkered primers containing restriction sites for HindIII and XbaI (Table S3) and cloned upstream of *GUS* coding region in the vector pBI121. The resulting plasmid was transformed into *Arabidopsis* (Col-0), and the T1 seeds were selected on kanamycin medium. The tissues from T2 transgenic plants were placed in the GUS substrate containing 50 mM sodium phosphate, pH 7.0, 0.1% Triton X-100, and 1 mM X-Gluc. After a 5 min vacuum infiltration, the samples were placed in a 37°C incubator. The leaf samples were embedded in 5% agarose and sectioned with a vibratome.

RNA Extraction and Northern Analyses

Small-scale extraction of RNA from one or two leaves was performed in the TRIzol reagent (Invitrogen, Gaihersburg, MD) following the manufacturer's instructions. Northern analyses and synthesis of random primed probes was carried out as described before (Kachroo et al., 2005).

Trypan Blue and Toluidine Blue Stainings

Leaf samples were taken from 2- or 4-week-old plants grown on soil. Trypan blue staining was performed as described earlier (Chandra-Shekara et al., 2006). Toluidine blue staining was carried out as described earlier (Tanaka et al., 2004).

SA, JA, FA, and Lipid Analyses

SA and SA glucoside (SAG) were extracted and measured from ~0.3 g of fresh weight leaf tissue, as described before (Chandra-Shekara et al., 2006).

FA analysis was done by placing leaf tissue in 2 ml of 3% H_2SO_4 in methanol. For JA extraction, leaves (1 g) were ground in liquid nitrogen and extracted in 100% methanol using dihydro-JA (DJA) as an internal standard. For lipid extraction, six to eight leaves were incubated at 75°C in isopropanol containing 0.001% BHT for ~15 min. To this, 1.5 ml chloroform and 0.6 ml water was added, and the samples were agitated at room temperature for 1 hr. The lipids were re-extracted in chloroform: methanol (2:1) until the leaves were bleached (see Supplemental Experimental Procedures for details).

SA, Glycerol, and JA Treatments

Glycerol, JA, and SA treatments were carried out by spraying 10–50 mM, 50 μM, or 500 μM solutions, respectively, prepared in sterile water. JA-treated plants were covered with a transparent plastic dome to maximize exposure to JA.

Pathogen Infection and Collection of Phloem Exudate

Inoculations with *Pseudomonas syringae* DC 3000 were conducted as described before (Kachroo et al., 2005). For analysis of SAR, the primary leaves were inoculated with $MgCl_2$ or the avirulent bacteria (10^7 cfu ml^{-1}), and 48 hr later the systemic leaves were inoculated with virulent bacteria (10^5 cfu ml^{-1}). Unless noted otherwise, samples from the systemic leaves were harvested at 3 and 6 dpi. Leaf exudate was collected as described earlier (Maldonado et al., 2002) (see Supplemental Data for details).

Analysis of Wax and Cutin Components and Cuticle Abrasion

For analysis of the wax component, 500 mg of 4-week-old leaves were immersed in 10 ml of chloroform for 10 s. An internal standard (100 μg of *n*-tetracosane) was added and the samples were derivatizated using 100 μl of *N,O*-bis(trimethylsilyl) fluoroacetamide (BSTFA) in 100 μl of pyridine, and the sealed tubes were incubated for 60 min at 90°C. The samples were again dried under a gentle stream of nitrogen and dissolved in 1 ml of hexane. Samples (1 μl) were injected into an HP-5 column of GC equipped with flame ionization detector.

Cutin monomer composition and content were determined using sodium methoxide-catalyzed transmethylation method followed by acetylation of the hydroxyl groups with acetic anhydride and GC-MS slightly modified from previously described (Molina et al., 2006) (see Supplemental Data for details).

Cuticle abrasion was carried out as described earlier with slight modifications (Campbell and McInnes, 1999). In brief, a solution containing bentonite (0.02%) and celite (1%) was gently rubbed on the leaf surface using cotton.

Microscopy, Chlorophyll Leaching, and Water Loss

For SEM analysis both abaxial and adaxial surface of the leaf samples was mounted on sample holder with 12 mm conductive carbon tabs (Ted Pella, Inc.), sputter-coated with gold-palladiim, and observed on a Hitachi S-3200 SEM with and without backscatter detector at 5 and 20 kV.

For TEM analysis leaves were fixed in paraformaldehyde and embedded in epon-araldite. Leaves were sectioned on a Reichert-Jung Ultracut E microtome with a Diatome diamond knife and observed under a Philips Tecnai Biotwin 12 TEM.

For chlorophyll-leaching assays, 100 mg of leaves were weighed and gently agitated, in the dark, at room temperature in tubes containing 80% ethanol (Lolle et al., 1997). Absorbance of each sample was measured at 664 and 647, and the micromolar concentration of total chlorophyll per gram of fresh weight was calculated using the following formula: total micromoles chlorophyll = 7.93 (A_{664}) + 19.3 (A_{647}).

For water loss measurements, 4-week-old plants were either subjected to drought or kept moist. The leaf weight was measured from ~50 leaves.

SUPPLEMENTAL DATA

Supplemental Data include seven figures, three tables, and Supplemental Experimental Procedures and can be found online at http://www.cell.com/cellhostandmicrobe/supplemental/S1931-3128(09)00026-2.

ACKNOWLEDGMENTS

We thank John Johnson for help with gas chromatography, Larry Rice for help with SEM, Mary Gail Engle for help with TEM, Claire Venard for help with thick sectioning, Rae-Dong Jeong for quantification of *R* gene levels, and Thomas Muse and Lev Orlov for help with fatty acid extractions and genotyping. We also thank Mike Pollard for cutin monomer spectra and useful advice, John Browse for *lacs2* and *lacs9* seeds, and Walter Grassmann for *Pseudomonas syringae* strain containing *AvrRPS4*. We thank Kansas Lipidomics Research Center Analytical Laboratory and its support from National Science Foundation's EPSCoR program, under grant number EPS-0236913 with matching support from the State of Kansas through Kansas Technology Enterprise Corporation and Kansas State University. This work was supported by grants from NSF (MCB#0421914), USDA-NRI (2004-03287), and KSEF (419-RDE-004, 04RDE-006, 820-RDE-007).

Received: July 10, 2008
Revised: October 14, 2008
Accepted: January 14, 2009
Published: February 18, 2009

Figure 6. Cuticle Phenotypes, SAR, and Basal Resistance in WT Plants Subjected to Mechanical Abrasion

(A) Toluidine blue-stained leaves from intact or treated plants.

(B) Transmission electron micrographs showing cuticle layer on adaxial surface of WT (Nössen) plants 1 and 24 hr post abrasion. Arrows indicate electron-opaque regions [scale bars, 100 nm (1 hr) and 50 nm (24 hr)].

(C) Analysis of lipid polyester monomer content of WT plants before and after 1 and 24 hr abrasion. Error bars represent SD.

(D) SAR in WT plants inoculated with $MgCl_2$ (mock) or *P. syringae* containing *AvrRPT2*. The distal leaves of a subset of plants were subjected to mechanical abrasion at 0, 12, 24, or 42 hr after inoculation of the avirulent pathogen in the primary leaves. The distal leaves in all plants were infiltrated with the virulent pathogen 48 hr after inoculation of the avirulent pathogen. Asterisks denote a significant difference with $MgCl_2$, 0 or 12 hr infiltrated leaves (t test, $p < 0.05$).

(E) Basal resistance in WT plants subjected to mechanical abrasion.

REFERENCES

Aubert, S., Gout, E., Bligny, R., and Douce, R. (1994). Multiple effects of glycerol on plant cell metabolism. J. Biol. Chem. *269*, 21420–21427.

Bessire, M., Chassot, C., Jacquat, A.-C., Humphry, M., Borel, S., Petétot, J.M.-C., Métraux, J.-P., and Nawrath, C. (2007). A permeable cuticle in *Arabidopsis* leads to a strong resistance to *Botrytis cinerea*. EMBO J. *26*, 2158–2168.

Bird, S.M., and Gray, J.E. (2003). Signals from the cuticle affect epidermal cell differentiation. New Phytol. *157*, 9–23.

Bonaventure, G., and Ohlrogge, J.B. (2002). Differential Regulation of mRNA Levels of Acyl Carrier Protein isoforms in Arabidopsis. Plant Physiol. *128*, 223–235.

Browse, J., and Somerville, C.R. (1991). Glycerolipid metabolism, biochemistry and regulation. Annu. Rev. Plant Physiol. Plant Mol. Biol. *42*, 467–506.

Campbell, C.S., and McInnes, K.J. (1999). Response of in situ leaf psychrometer to cuticle removal by abrasion. Agron. J. *91*, 859–862.

Cao, H., Bowling, S.A., Gordon, A.S., and Dong, X. (1994). Characterization of an Arabidopsis mutant that is nonresponsive to inducers of systemic acquired resistance. Plant Cell *6*, 1583–1592.

Chanda, B., Venugopal, S.C., Kulshrestha, K., Navarre, D., Downie, B., Kachroo, A., and Kachroo, P. (2008). Glycerol-3-phosphate levels are associated with basal resistance to the hemibiotrophic fungus *Colletotrichim higginsianum* in Arabidopsis. Plant Physiol. *140*, 2017–2029.

Chandra-Shekara, A.C., Gupte, M., Navarre, D.A., Raina, S., Raina, R., Klessig, D., and Kachroo, P. (2006). Light-dependent hypersensitive response and resistance signaling to turnip crinkle virus in Arabidopsis. Plant J. *45*, 320–335.

Chandra-Shekara, A.C., Venugopal, S.C., Barman, S.R., Kachroo, A., and Kachroo, P. (2007). Plastidial fatty acid levels regulate resistance gene-dependent defense signaling in Arabidopsis. Proc. Natl. Acad. Sci. USA *104*, 7277–7282.

Clough, S.J., and Bent, A.F. (1998). Floral dip: a simplified method for Agrobacterium -mediated transformation of *Arabidopsis thaliana*. Plant J. *16*, 735–743.

Durrant, W.E., and Dong, X. (2004). Systemic acquired resistance. Annu. Rev. Phytopathol. *42*, 185–209.

Glazebrook, J. (2005). Contrasting mechanisms of defense against biotrophic and necrotrophic pathogens. Annu. Rev. Phytopathol. *43*, 205–227.

Gray, W.M. (2002). Plant defence: a new weapon in the arsenal. Curr. Biol. *12*, R352–R354.

Guerra, D.J., Ohlrogge, J.B., and Frantzen, M. (1986). Activity of acyl carrier protein isoforms in reaction of plant fatty acid metabolism. Plant Physiol. *82*, 448–453.

Heidel, A.J., Clarke, J.D., Antonovics, J., and Dong, X. (2004). Fitness costs of mutations affecting the systemic acquired resistance pathway in *Arabidopsis thaliana*. Genetics *168*, 2197–2206.

Heil, M., and Baldwin, I.T. (2002). Fitness costs of induced resistance: emerging experimental support for a slippery concept. Trends Plant Sci. *7*, 61–66.

Kachroo, P., Shanklin, J., Shah, J., Whittle, E., and Klessig, D. (2001). A fatty acid desaturase modulates the activation of defense signaling pathways in plants. Proc. Natl. Acad. Sci. USA *98*, 9448–9453.

Kachroo, A., Lapchyk, L., Fukushigae, H., Hildebrand, D., Klessig, D., and Kachroo, P. (2003). Plastidial fatty acid signaling modulates salicylic acid- and jasmonic acid-mediated defense pathways in the Arabidopsis *ssi2* mutant. Plant Cell *12*, 2952–2965.

Kachroo, A., Venugopal, S.C., Lapchyk, L., Falcone, D., Hildebrand, D., and Kachroo, P. (2004). Oleic acid levels regulated by glycerolipid metabolism modulate defense gene expression in Arabidopsis. Proc. Natl. Acad. Sci. USA *101*, 5152–5157.

Kachroo, A., Shanklin, J., Whittle, E., Lapchyk, L., Hildebrand, D., and Kachroo, P. (2007). The *Arabidopsis* stearoyl-acyl carrier protein-desaturase family and the contribution of leaf isoforms to oleic acid synthesis. Plant Mol. Biol. *63*, 257–271.

Kachroo, A., Daqi, F., Havens, W., Navarre, D., Kachroo, P., and Ghabrial, S. (2008). An oleic acid–mdiated pathway induces constitutive defense signaling and enhanced resistance to multiple pathogens in soybean. Mol. Plant Microbe Interact. *21*, 564–575.

Kachroo, P., Venugopal, S.C., Navarre, D.A., Lapchyk, L., and Kachroo, A. (2005). Role of salicylic acid and fatty acid desaturation pathways in *ssi2*-mediated signaling. Plant Physiol. *139*, 1717–1735.

Kachroo, A., and Kachroo, P. (2006). Salicylic acid-, jasmonic acid- and ethylene-mediated regulation of plant defense signaling. Genet. Eng. *28*, 55–83.

Kumar, D., and Klessig, D.F. (2003). The high-affinity salicylic acid-binding protein 2 is required for plant innate immunity and has salicylic acid-stimulated lipase activity. Proc. Natl. Acad. Sci. USA *100*, 16101–16106.

Kunst, L., Browse, J., and Somerville, C. (1988). Altered regulation of lipid biosynthesis in a mutant of Arabidopsis deficient in chloroplast glycerol-3-phosphate acyltransferase activity. Proc. Natl. Acad. Sci. USA *85*, 4143–4147.

Li, Y., Beisson, F., Koo, A.J., Molina, I., Pollard, M., and Ohlrogge, J. (2007). Identification of acyltransferases required for cutin biosynthesis and production of cutin with suberin-like monomers. Proc. Natl. Acad. Sci. USA *104*, 18339–18344.

Lolle, S.J., and Pruitt, R.E. (1999). Epidermal cell interactions: a case for local talk. Trends Plant Sci. *4*, 14–20.

Lolle, S.J., Berlyn, G.P., Engstrom, E.M., Krolikowski, K.A., Reiter, W.D., and Pruitt, R.E. (1997). Developmental regulation of cell interactions in the Arabidopsis *fiddlehead-1* mutant: a role for the epidermal cell wall and cuticle. Dev. Biol. *189*, 311–321.

Maldonado, A.M., Doerner, P., Dixon, R.A., Lamb, C.J., and Cameron, R.K. (2002). A putative lipid transfer protein involved in systemic resistance signaling in Arabidopsis. Nature *419*, 399–403.

Molina, I., Bonaventure, G., Ohlrogge, J., and Pollard, M. (2006). The lipid polyester composition of *Arabidopsis thaliana* and *Brassica napus* seeds. Phytochemistry *67*, 2597–2610.

Nandi, N., Welti, R., and Shah, J. (2004). The *Arabidopsis thaliana* dihydroxyacetone phosphate reductase gene suppressor of fatty acid desaturase deficiency1 is required for glycerolipid metabolism and for the activation of systemic acquired resistance. Plant Cell *16*, 465–477.

Park, S.-W., Kaimoyo, E., Kumar, D., Mosher, S., and Klessig, D. (2007). Methyl salicylate is a critical mobile signal for plant systemic acquired resistance. Science *318*, 113–116.

Pollard, M., Beisson, F., Li, Y., and Ohlrogge, J.B. (2008). Builiding lipid barriers: biosynthesis of cutin and suberin. Trends Plant Sci. *13*, 236–246.

Rasmussen, J.B., Hammerschmidt, R., and Zook, M.N. (1991). Systemic induction of salicylic acid accumulation in cucumber after inoculation with *Pseudomonas syringae* pv *syringae*. Plant Physiol. *97*, 1342–1347.

Riederer, M. (2006). Introduction: Biology of the plant cuticle. In Biology of the Plant Cuticle, M. Riederer and C. Muller, eds. (Oxford, UK: Blackwell publishers), pp. 1–8.

Samuels, L., Kunst, L., and Jetter, R. (2008). Sealing plant surfaces: Cuticular wax formation by epidermal cells. Annu. Rev. Plant Biol. *59*, 683–707.

Schnurr, J., Shockey, J., deBoer, G.-J., and Browse, J. (2002). Fatty acid export from the chloroplast: Molecular characterization of a major plastidial acyl-coenzymeA synthetase from Arabidopsis. Plant Physiol. *129*, 1700–1709.

Schnurr, J., Shockey, J., and Browse, J. (2004). The acyl-CoA synthetase encoded by LACS2 is essential for normal cuticle development in *Arabidopsis*. Plant Cell *16*, 629–643.

Seskar, M., Shulaev, V., and Raskin, I. (1998). Endogenous methyl salicylate in pathogen-inoculated tobacco plants. Plant Physiol. *116*, 387–392.

Shockey, J., Fulda, M., and Browse, J. (2002). Arabidopsis contains nine long-chain acyl-coenzymeA synthetases that participate in fatty acid and glycerolipid metabolism. Plant Physiol. *129*, 1710–1722.

Smith-Becker, J., Marois, E., Huguet, E.J., Midland, S.L., Sims, J.J., and Keen, N.T. (1998). Accumulation of salicylic acid and 4-hydroxybenzoic acid in phloem of cucumber during systemic acquired resistance is preceded by a transient increase in phenylalanine ammonia-lyase activity in petioles and stems. Plant Physiol. *116*, 231–238.

Somerville, C., and Browse, J. (1991). Plant lipids: metabolism, mutants, and membranes. Science *252*, 80–87.

Suh, M.C., Schultz, D.J., and Ohlrogge, J.B. (1999). Isoforms of acyl carrier protein involved in seed-specific fatty acid synthesis. Plant J. *17*, 679–688.

Tanaka, T., Tanaka, H., Machida, C., Watanabe, M., and Machida, Y. (2004). A new method for rapid visualization of defects in leaf cuticle reveals five intrinsic patterns of surface defects in Arabidopsis. Plant J. *37*, 139–146.

Tanaka, H., and Machida, Y. (2006). The cuticle and cellular interactions. In Biology of the Plant Cuticle, M. Riederer and C. Muller, eds. (Oxford, UK: Blackwell publishers), pp. 312–333.

Tang, D., Simonich, M.T., and Innes, R.W. (2007). Mutations in *LACS2*, a Long-Chain Acyl-Coenzyme A Synthetase, enhance susceptibility to avirulent *Pseudomonas syringae* but confer resistance to *Botrytis cinerea* in Arabidopsis. Plant Physiol. *144*, 1093–1103.

Thomma, B.P., Penninckx, I.A., Broekaert, W.F., and Cammue, B.P. (2001). The complexity of disease signaling in Arabidopsis. Curr. Opin. Immunol. *13*, 63–68.

Truman, W., Bennett, M.H., Kubigsteltig, I., Turnbull, C., and Grant, M. (2007). Arabidopsis systemic immunity uses conserved defense signaling pathways and is mediated by jasmonates. Proc. Natl. Acad. Sci. USA *104*, 1075–1080.